Magnetoresistance in quantum wires: Boundary-roughness scattering

H. Akera and T. Ando
Institute for Solid State Physics, University of Tokyo, 7-22-1 Roppongi, Minato-ku, Tokyo 106, Japan
(Received 14 December 1990)

A quantum-mechanical calculation of the magnetoresistance of quantum wires is performed in the presence of boundary-roughness scattering. The roughness is described by two parameters—the root-mean-square deviation and the correlation length—and the Boltzmann transport equation is used. The roughness scattering gives rise to a strong positive magnetoresistance when the wire width is larger and the correlation length smaller than the Fermi wavelength. When the confining potential is varied from hard wall to parabolic, the magnetoresistance is shown to have a sharper peak for softer confinement. A numerical study based on Landauer's formula is also performed. The localization effect present in weak magnetic fields tends to suppress the positive magnetoresistance in narrow wires but becomes less important with the increase of the wire width.

I. INTRODUCTION

Recent developments in microfabrication technology have made it possible to obtain quantum wires by introducing a confining potential in a two-dimensional electron system. A typical sample is made on a modulation-doped $GaAs/Al_xGa_{1-x}As$ heterostructure by the etching or split-gate techniques. Because of a long mean free path compared with the wire width, a number of new transport phenomena related to wire junctions have been observed, such as anomalies in the low-field Hall effect,[1-3] a bend resistance,[4] and a negative resistance.[5] Quite recently, the magnetoresistance of long wires has been measured,[6] in which scattering from boundary roughness has a stronger effect on the transport. Such quantum wires exhibit a large positive magnetoresistance. A similar magnetoresistance has been observed in aluminum films[7] and explained by a classical-trajectory model.[8-11] However, if the wire width is comparable to the Fermi wavelength, strong quantum size effects are expected. The purpose of the present paper is to study effects of boundary roughness in such quantum wires.

The classical theory[12] assumes that each electron follows a classical trajectory with the Fermi velocity and is reflected specularly with the probability p and otherwise scattered into a random direction. This electron-trajectory model has been applied to study the magnetoresistance in metallic films.[13,14] In the absence of a magnetic field, the roughness itself cannot produce a nonzero resistivity because straight trajectories parallel to film surfaces have an infinite mean free path and dominate the current. In the presence of a magnetic field, the resistivity becomes nonzero because all electrons follow a curved trajectory and are scattered at a collision with the boundaries. When the cyclotron radius R_c becomes smaller than half of the film thickness W, the resistivity vanishes again because of the absence of backscattering. A detailed numerical calculation[15] performed for $p=0$ has shown that the resistivity increases with the magnetic field at low fields, exhibits a maximum at $W/R_c \approx 0.55$, and decreases down to the bulk resistivity at $W/R_c = 2$.

Quantum-mechanical calculations have been reported of the resistivity of films in the absence of a magnetic field.[16-18] The roughness has been described by two parameters: the root-mean-square deviation of film boundaries and its correlation length along the film surface. Calculations have recently been extended to consider effects of the magnetic field classically in the transport equation.[19] The roughness scattering also plays an important role in other systems and some quantum-mechanical studies have been performed. In a study of the microwave surface impedance of metals in magnetic fields, the lifetime of a magnetic surface state due to roughness scattering has been discussed.[20] In a Si inversion layer, roughness at the $Si-SiO_2$ interface is one of the main scattering mechanisms for the electron transport parallel to the interface.[21] Their effects on the mobility have been investigated by several authors.[22-27] Studies on the mobility in quantum-well structures have also been performed.[28-30]

Effects of boundary roughness on the current distribution and the Hall effect have been studied in quantum wires.[31] It has been noted that the boundary roughness can cause a peculiar current distribution among subbands, giving rise to a considerable suppression of the weak-field Hall resistance. In this paper the magnetoresistance is calculated in quantum wires in the presence of boundary-roughness scattering. By solving the Boltzmann transport equation, the dependence of the resistivity on the wire width, the correlation length, and the shape of the confining potential is studied in detail. In Sec. II the model is introduced and the method of calculation is briefly described. In Sec. III numerical results are presented after a brief description of the analytic treatment for some limiting cases. In Sec. IV a numerical study is performed with the use of Landauer's conductance formula[32] for finite-length wires. Summary and conclusion are given in Sec. V.

II. MODEL AND METHOD

A. Hamiltonian

Consider a noninteracting two-dimensional system confined in a wire in the xy plane. In the presence of a magnetic field H perpendicular to the system, the Hamiltonian is given by

$$\mathcal{H}=\frac{1}{2m}\left[\mathbf{p}+\frac{e}{c}\mathbf{A}\right]^2+V(y)\ , \tag{1}$$

where m is the effective mass, $e>0$, and $\mathbf{A}=(-Hy,0)$. The spin Zeeman splitting is completely neglected and the confining potential is assumed to be as follows:

$$V(y)=\begin{cases}\frac{1}{2}m\omega_e^2(y+\frac{1}{2}W_0)^2 & \text{if } y<-\frac{1}{2}W_0\\ 0 & \text{if } -\frac{1}{2}W_0<y<\frac{1}{2}W_0\\ \frac{1}{2}m\omega_e^2(y-\frac{1}{2}W_0)^2 & \text{if } y>\frac{1}{2}W_0\ .\end{cases} \tag{2}$$

A self-consistent calculation of energy levels in wires made at a split-gate GaAs/$Al_xGa_{1-x}As$ heterostructure[33] has shown that the confining potential is close to the above form and ω_e depends only a little on the wire width. Experimental data of the quantized conductance of ballistic narrow channels also support this choice of the confining potential.[34] Each eigenstate can be specified by the subband index $n=1,2,\ldots$ and the wave vector k along the wire.

There can be various ways to define an effective width in such a confining potential.[35] Here we define an effective width using the classical turning point of an electron traveling along the y direction with energy corresponding to half of the Fermi energy. We have

$$W=W_0+2y_e\ , \tag{3}$$

with

$$\frac{1}{2}m\omega_e^2y_e^2=\frac{1}{2}\frac{\hbar^2k_F^2}{2m}\ , \tag{4}$$

with the Fermi wave number k_F. A hard-wall potential is obtained when ω_e becomes infinitely large.

B. Transport equation

We shall use the Boltzmann transport equation to calculate the resistivity and therefore neglect any localization effects and fluctuations. The Boltzmann equation in a quantum wire is[36]

$$\frac{\partial g_{nk}}{\partial t}+v_{nk}\frac{\partial g_{nk}}{\partial x}+\frac{e}{\hbar}\frac{\partial\phi}{\partial x}\frac{\partial g_{nk}}{\partial k}=\sum_{n',k'}W_{n'k'nk}(g_{n'k'}-g_{nk})\ , \tag{5}$$

where g_{nk} and v_{nk} are the distribution function and the group velocity, respectively, of a state with wave number k in the nth subband and ϕ is the scalar potential. The scattering probability $W_{n'k'nk}$ has the symmetry of the detailed balance $W_{n'k'nk}=W_{nkn'k'}$ and is given in the Born approximation by

$$W_{n'k'nk}=\frac{2\pi}{\hbar}\langle|U_{n'k'nk}|^2\rangle_{\rm av}\delta(\varepsilon_{n'k'}-\varepsilon_{nk})\ , \tag{6}$$

where ε_{nk} is the eigenenergy, $U_{n'k'nk}$ the matrix element of the scattering potential, and $\langle\cdots\rangle_{\rm av}$ means taking the average over configurations of scatterers. We assume that the scalar potential is described by a static and uniform electric field E along the wire: $\phi=-Ex$. Retaining only the first-order correction in E and writing

$$g_{nk}=f(\varepsilon_{nk})+eEv_{nk}\tau_{nk}\frac{\partial f}{\partial\varepsilon}(\varepsilon_{nk})\ , \tag{7}$$

with $f(\varepsilon)$ the Fermi distribution function, we have the following set of equations, which determine the relaxation time $\tau_n(\varepsilon)$ or the mean free path $l_n(\varepsilon)=v_n\tau_n$:

$$\sum_{n'=1}^{N}(K_{n-n'+}-K_{n+n'+})l_{n'}(\varepsilon)=1\quad(n=1,2,\ldots,N)\ , \tag{8}$$

where N is the number of subbands giving propagating waves at ε and $n\pm$ denotes such a channel with velocity $v_{n\pm k}=\pm v_n$ for $\varepsilon_{n\pm k}=\varepsilon$. Further, $K_{\beta\alpha}$ is the "transition rate per unit length" between channels α and β, defined by

$$K_{\beta\alpha}=\begin{cases}\langle|U_{\beta\alpha}|^2\rangle_{\rm av}(L/\hbar^2|v_\alpha v_\beta|) & \text{if } \beta\neq\alpha\\ -\sum_{\gamma(\neq\alpha)}K_{\gamma\alpha} & \text{if } \beta=\alpha\ ,\end{cases} \tag{9}$$

which satisfies $K_{\alpha\beta}=K_{\beta\alpha}$ from the condition of the detail balance. The conductivity is given by

$$\sigma=-\frac{2e^2}{L}\sum_{n,k}v_{nk}^2\tau_{nk}\frac{\partial f}{\partial\varepsilon}(\varepsilon_{nk})=\int d\varepsilon\left[-\frac{\partial f}{\partial\varepsilon}\right]\sigma(\varepsilon)\ , \tag{10}$$

with

$$\sigma(\varepsilon)=\frac{4e^2}{h}\sum_{n=1}^{N}l_n(\varepsilon)\ , \tag{11}$$

where L is the wire length.

C. Boundary roughness

In general, boundary roughness[21] is described by deviations of boundaries, $\Delta_\pm(x)$, at $y=\pm W_0/2$ and modulations in the strength of the potential, i.e., a variation of $\omega_{e\pm}$ along the wire direction:

$$V(x,y)=\begin{cases}\frac{1}{2}m\omega_{e-}(x)^2(y-y_-)^2 & \text{if } y<y_-\\ 0 & \text{if } y_-<y<y_+\\ \frac{1}{2}m\omega_{e+}(x)^2(y-y_+)^2 & \text{if } y>y_+\end{cases} \tag{12}$$

with

$$y_\pm=\pm\frac{W_0}{2}+\Delta_\pm(x)\ . \tag{13}$$

In this paper it is assumed that $\omega_{e\pm}(x)=\omega_e$ because the self-consistent calculation[33] shows that ω_e depends only a

little on the wire width. Further, $\Delta_{\pm}(x)$ is assumed to be small compared with the Fermi wavelength $\lambda_F=2\pi/k_F$. By taking into account terms in the lowest order of $\Delta_{\pm}(x)$, the matrix element of the perturbation is given by

$$(n'k'|\mathcal{H}'_{\pm}|nk)=\frac{\hbar^2}{2m}Y^{\pm}_{n'k'nk}\frac{1}{L}\times\int dx\,\Delta_{\pm}(x)\exp[i(k-k')x] \tag{14}$$

with

$$Y^{\pm}_{n'k'nk}=\mp\frac{2m}{\hbar^2}\int_{\pm W_0/2}^{\pm\infty}dy\,\eta_{n'k'}\frac{\partial V}{\partial y}\eta_{nk}\ , \tag{15}$$

where η_{nk} is the wave function for the motion along y. It is shown in the Appendix that in the case of the hard-wall potential ($\omega_e\to\infty$) the above integral leads to the well-known expression[21]

$$Y^{\pm}_{n'k'nk}=\mp\frac{\partial\eta_{n'k'}}{\partial y}\frac{\partial\eta_{nk}}{\partial y}\bigg|_{\pm W/2}\ . \tag{16}$$

The roughness is conventionally characterized by the root-mean-square deviation Δ and the correlation length Λ defined by

$$\begin{aligned}&\langle\Delta_+(x)\rangle=\langle\Delta_-(x)\rangle=\langle\Delta_+(x)\Delta_-(x')\rangle=0\ ,\\&\langle\Delta_+(x)\Delta_+(x')\rangle=\langle\Delta_-(x)\Delta_-(x')\rangle\\&\qquad=\Delta^2\exp\left[-\frac{(x-x')^2}{\Lambda^2}\right]\ .\end{aligned} \tag{17}$$

Within the Born approximation we obtain the following expression of the transition rate:

$$K_{\beta\alpha}=\frac{\sqrt{\pi}}{4}\left[\frac{\hbar}{m}\right]^2\Lambda\Delta^2\frac{(Y^+_{\beta\alpha})^2+(Y^-_{\beta\alpha})^2}{v_\beta v_\alpha}\times\exp[-\tfrac{1}{4}\Lambda^2(k_\beta-k_\alpha)^2]\ . \tag{18}$$

III. RESULTS

A. Positive magnetoresistance

In the absence of a magnetic field and in the case of small correlation length $\Lambda\ll\lambda_F$, we can easily solve Eq. (8) since $K_{n-n'+}=K_{n+n'+}$ and have

$$\tau_n^{-1}=v_n(K_{n-n+}-K_{n+n+})=2v_n\sum_{n'=1}^{N}K_{n'-n+}\ . \tag{19}$$

In the case of the hard-wall potential, we have

$$\frac{1}{\tau_n}=\pi^{5/2}v_F\frac{\Lambda\Delta^2}{\lambda_F^4}\left[\frac{\lambda_F}{W}\right]^6 n^2\sum_{m=1}^{N}\frac{v_F}{v_m}m^2\ , \tag{20}$$

since $|Y^{\pm}_{n'k'nk}|=2\pi^2n'n/W^3$. The relaxation time is proportional to $1/n^2$, i.e., the roughness is not effective in the lower subbands. In a vanishing magnetic field the conductivity is dominated by the current carried by the lowest subbands having long relaxation time or long mean free path. This is closely related to the vanishing of the resistivity at $H=0$ in the classical-trajectory model.

When the number of occupied subbands ($\approx 2W/\lambda_F$) is sufficiently large, the replacement of the summation over n by an integral gives

$$\frac{1}{\tau_n}\simeq 2\pi^{7/2}v_F\frac{\Lambda\Delta^2}{\lambda_F^4}\left[\frac{\lambda_F}{W}\right]^3 n^2 \tag{21}$$

and

$$\frac{\sigma}{W}\simeq\frac{1}{3\pi^{3/2}}\frac{e^2}{h}\frac{\lambda_F^3}{\Lambda\Delta^2}\left[\frac{W}{\lambda_F}\right]^2\ . \tag{22}$$

In the presence of a weak magnetic field, electrons in the lower subbands start to suffer from roughness scatterings due to the large Lorentz force. Therefore, the strong dependence of the relaxation time on the subband disappears and every subband is almost equally affected by scatterings, leading to a reduction in the conductivity, i.e., a positive magnetoresistance. A rough estimate of the conductivity near the resistance peak ($W\sim 0.5R_c$) can be made if we assume that each subband has a relaxation time τ obtained by the average of the zero-field scattering rates over the occupied subbands:

$$\frac{1}{\tau}=\left\langle\frac{1}{\tau_n(H=0)}\right\rangle\simeq\frac{2^3\pi^{7/2}}{3}v_F\frac{\Lambda\Delta^2}{\lambda_F^4}\frac{\lambda_F}{W}\ , \tag{23}$$

where the last equality holds for $W/\lambda_F\gg 1$. In this case, we have

$$\frac{\sigma}{W}\simeq\frac{3}{4\pi^{5/2}}\frac{e^2}{h}\frac{\lambda_F^3}{\Lambda\Delta_2}\frac{W}{\lambda_F}\ . \tag{24}$$

This formula shows that near the peak resistivity σ/W increases linearly with the width. The classical calculation[11] for $p=0$ predicts a linear dependence at the resistance peak, giving roughly $\sigma/W\sim(10e^2/h)W/\lambda_F$. The comparison with Eq. (24) suggests that $\Lambda\Delta^2/\lambda_F^3\propto 1-p$. Equation (22) shows that σ/W at $H=0$ increases quadratically with the width. In the limit $W/\lambda_F\to\infty$, σ/W^2 at the vanishing field diverges while it remains finite at nonzero magnetic fields, in agreement with the classical result.

Approximate expressions can be derived also for parabolic confinement, i.e., for $y_e=W/2$. In this case, the matrix element of the roughness, Eq. (15), is appreciable only among subbands that are close to each other in energy. By replacing the velocity $v_{n'}$ appearing in Eq. (19) by v_n and making use of

$$\sum_{n'=1}^{\infty}|Y_{nn'}|^2=4\xi^{-8}\int_0^\infty dy\,y^2\eta_n(y)^2=\xi^{-6}(2n-1) \tag{25}$$

with $\xi=(W\lambda_F/2\sqrt{2}\pi)^{1/2}$, we have

$$\frac{1}{\tau_n}\simeq 2^{5/2}\pi^{3/2}v_F\frac{\Lambda\Delta^2}{\lambda_F^4}\left[\frac{\lambda_F}{W}\right]^3(2n-1)\frac{v_F}{v_n}\ . \tag{26}$$

In the limit $W/\lambda_F\gg 1$, we have for $H=0$

$$\frac{\sigma}{W}\simeq\frac{1}{2^{3/2}\pi^{3/2}}\frac{e^2}{h}\frac{\lambda_F^3}{\Lambda\Delta^2}\left[\frac{W}{\lambda_F}\right]^2\ln\left[\frac{2W}{\lambda_F}\right] \tag{27}$$

and for $H \neq 0$

$$\frac{\sigma}{W} \simeq \frac{1}{2^{7/2}\pi^{1/2}} \frac{e^2}{h} \frac{\lambda_F^3}{\Lambda\Delta^2} \left[\frac{W}{\lambda_F} \right]^2 . \quad (28)$$

These formulas show that the positive magnetoresistance becomes less prominent in the case of the soft-wall confining potential. Note also that the dependence on the width is different from that in the case of the hard-wall confining potential both for $H=0$ and $H>0$.

When the correlation length is nonzero, the wave-number change at each scattering is limited to the order Λ^{-1} due to the exponential factor in Eq. (18). At correlation lengths comparable to the Fermi wavelength, forward scattering among subbands is dominant and backscattering is suppressed considerably. Therefore, the mean free path of all subbands is determined by the rate of the largest backscattering which occurs within the highest occupied subband. This backscattering rate remains the same up to the field corresponding to $W/R_c \sim 0.5$, because the Lorentz force acting on electrons in the highest subband is small due to its small velocity along the wire. Consequently all subbands give almost equal contributions to the current and only a small positive magnetoresistance is expected.

The essential ingredient of this positive magnetoresistance is that the conductivity is a sum of the mean free paths of each subband and is essentially determined by the longest mean free path. There is another formula for the resistivity using a memory function used frequently.[37,38] If it is applied to a multisubband case, the current is, roughly speaking, proportional to τ given by Eq. (23). Therefore, this memory-function approach gives no positive magnetoresistance.

B. Examples

In the examples shown in the following, the magnetic field is varied with fixed Fermi energy $E_F=(\hbar k_F)^2/2m$. Calculated results are functions of the following five parameters: the wire width W/λ_F, the correlation length Λ/λ_F, the width of the edge regions y_e/W, the strength of the magnetic field H, and the temperature k_BT/E_F. The conductivity σ is plotted in units of $(e^2/h)\lambda_F^4/\Lambda\Delta^2$. The magnetic field is measured in units of mcv_F/eW or by the ratio of the wire width and the cyclotron radius.

Figure 1 presents the calculated energy dependence of the contribution of each subband to the conductivity for wire width $W/\lambda_F=3$ confined by a hard-wall potential in the absence of a magnetic field and at the magnetic field corresponding to $W/R_c=0.5$. The correlation length is assumed to be vanishingly small, i.e., $\Lambda \ll \lambda_F$. The singular one-dimensional density of states causes a vanishing conductivity because of the divergence in the probability of scattering to the highest subband when the energy is just at its bottom. This gives rise to a quantum oscillation of the resistivity when the magnetic field is varied. When the energy is away from subband bottoms, the contribution of subband n is proportional to $v_n/n^2 (\sim v_F/n^2)$ and is largest for the lowest subband at zero field, as discussed in the preceding section. In the presence of a magnetic field, such a strong dependence on the subband index disappears and every subband carries almost an equal amount of the current.

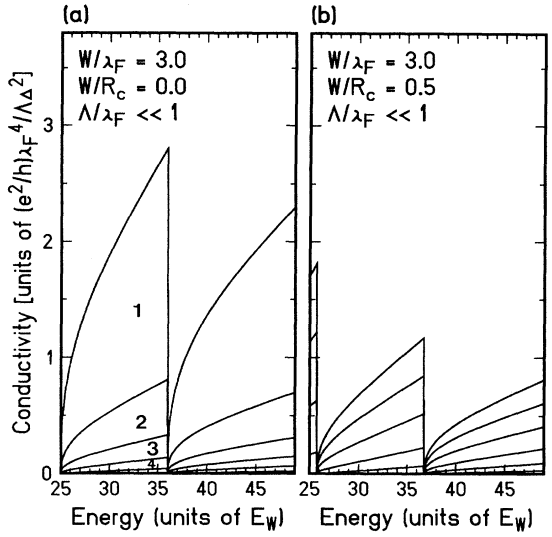

FIG. 1. Calculated conductivity as a function of energy for a wire width $W=3\lambda_F$ and a hard-wall potential when the correlation length of roughness is much shorter than λ_F (a) in the absence of a magnetic field and (b) at the magnetic field satisfying $W=0.5R_c$. The Fermi energy is at $36E_W$ with $E_W=(\hbar^2/2m)(\pi/W)^2$ and six subbands are occupied by electrons at zero temperature. Contributions from each subband ($n=1,2,\ldots$) are also shown.

The corresponding results for a large correlation length are given in Fig. 2. The current is carried by different subbands almost equally at both vanishing and nonzero magnetic field. Note that the reduction in the conductivity near the bottom of each subband is strongly

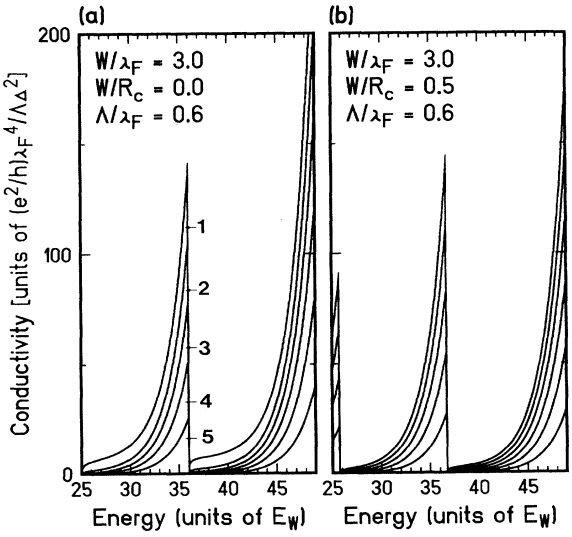

FIG. 2. Calculated conductivity as a function of energy at the correlation length $\Lambda=0.6\lambda_F$.

enhanced in comparison with the case of short-range roughness. The backscattering rate within the highest occupied subband drops considerably when the energy is away from its bottom. It can be concluded that the long-range boundary roughness tends to make the amplitude of the quantum oscillation larger.

A recent self-consistent Thomas-Fermi calculation in a split-gate device shows that density fluctuations of ionized donors give a roughness with a correlation length larger than the Fermi wavelength.[39] A roughness can also be produced by deviations of a line drawn by the lithography technique, but no roughness with short correlation lengths is expected because such a line is drawn several hundred angstroms away from the two-dimensional electron system. So far, wires exhibiting a clear positive magnetoresistance have been made by ion exposure[6] and may contain short-range roughness due to damage of the crystal structure.

The magnetic-field dependence of the resistivity is presented in Fig. 3 when the temperature is zero. The positive magnetoresistance is accompanied by quantum oscillations reflecting the density of states. At larger magnetic fields the resistivity decreases due to the formation of edge states. As the temperature increases (Fig. 4), the quantum oscillations are smeared out and the positive magnetoresistance is more clearly seen. For short correlation lengths and moderate temperatures, the resistivity exhibits a behavior similar to the classical calculations[15,11] and the experiments.[6] At correlation lengths larger than $0.6\lambda_F$ magnetoresistance disappears.

At higher temperatures, the resistivity drops abruptly at high magnetic fields ($W/R_c \gtrsim 1.3$ at $k_BT/E_F=0.06$). Electrons near the bottom of the lowest few subbands have extremely long mean free paths because they are subject to weak backscattering. Such well-defined edge states start to participate in the current and give a large conductivity at high temperatures.

Figure 5(a) presents calculated results of the resistivity as a function of the magnetic field for a wider wire width $W/\lambda_F=5.5$ at $k_BT/E_F=0.02$. As the number of subbands increases, the resistivity dip at $H=0$ becomes deeper and sharper. Such strong width dependence of the low-field behavior has been reported also in the resistivity of films.[19] When the number of subbands decreases down to one, the resistivity becomes a decreasing function of the magnetic field even at the vanishing correlation length, as shown in Fig. 5(b).

The conductivity divided by the wire width, or the averaged two-dimensional conductivity, is plotted as a function of the width for $\Lambda \ll \lambda_F$ in Fig. 6. The value at the vanishing magnetic field shows a parabolic dependence on the width with quantum oscillations, while that at $W/R_c=0.5$ shows a linear dependence. A crossover occurs at $W/\lambda_F \sim 1$. The analytic expressions (22) and (24) are also given in the figure and explain the numerical results quite well.

Figure 7 shows how the shape of the confining potential affects the magnetoresistance. The effective width is fixed at $W/\lambda_F=3$ and the percentage of the edge region with potential gradient, y_e/W, is varied. As y_e/W becomes larger, the resistivity at the peak decreases because roughness scattering becomes weaker at a fixed Δ and Λ. The ratio of the zero-field resistivity to the peak does not change much except in the very vicinity of $y_e/W=0.5$.

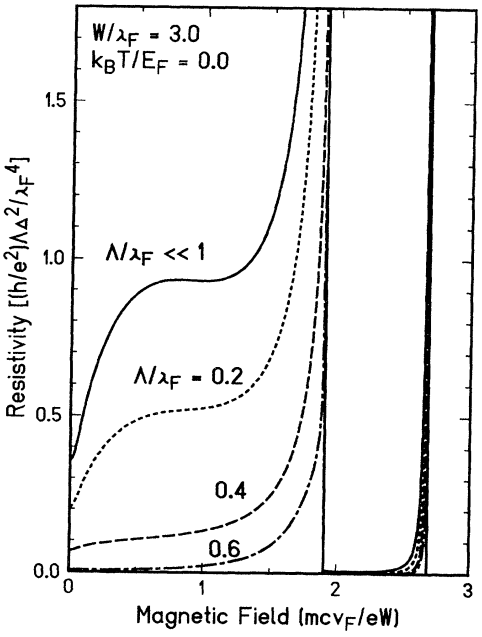

FIG. 3. Calculated magnetoresistance for wires with width $W/\lambda_F=3$ at absolute zero for several correlation lengths. Along the horizontal axis the ratio of the wire width and the cyclotron radius is plotted.

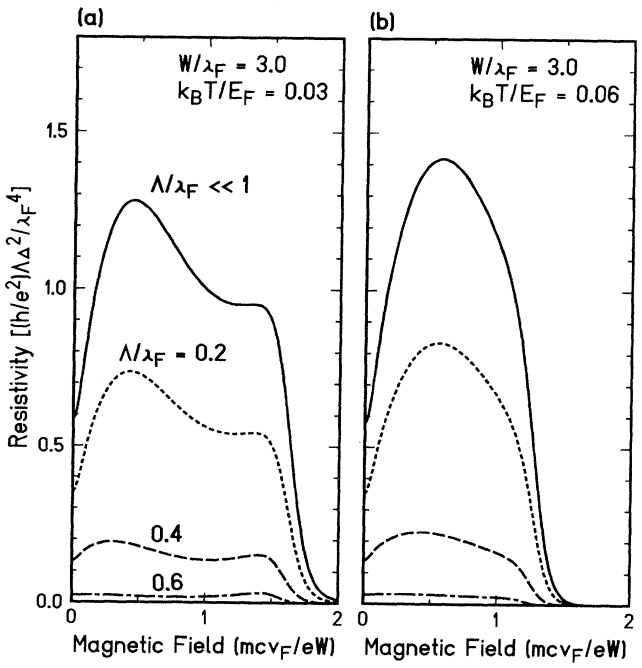

FIG. 4. Calculated magnetoresistance for wires with width $W/\lambda_F=3$ at temperatures (a) $k_BT/E_F=0.03$ and (b) 0.06.

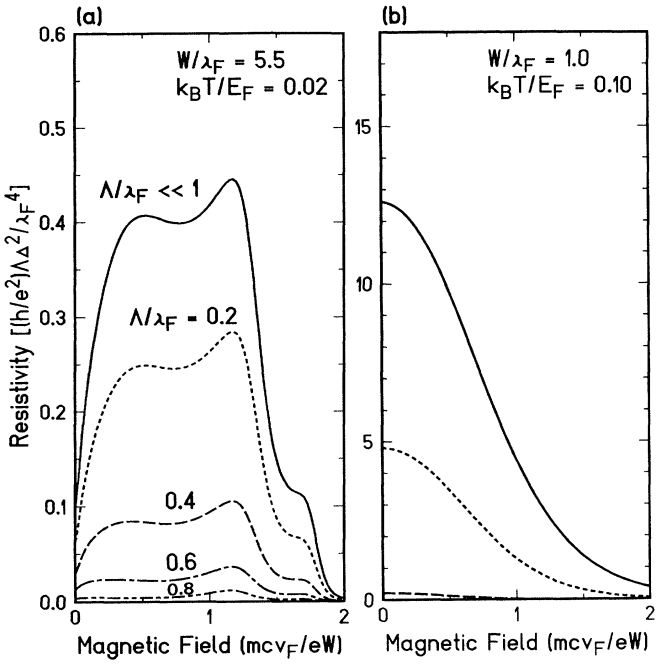

FIG. 5. Calculated magnetoresistance for wires with width (a) $W/\lambda_F=5.5$ and (b) $W/\lambda_F=1$.

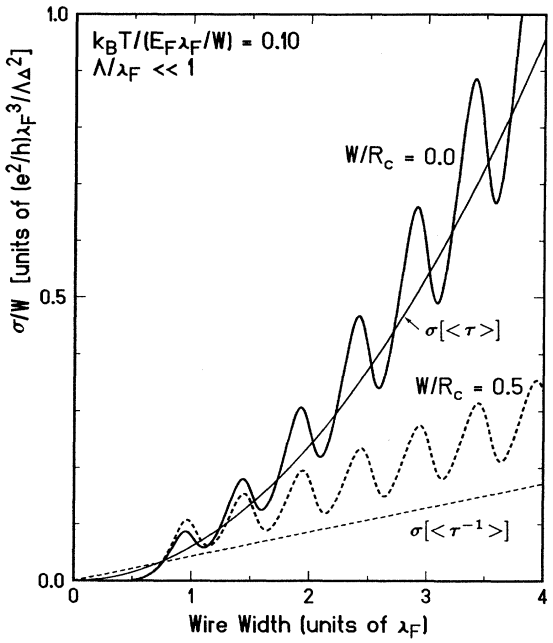

FIG. 6. Width dependence of conductivity. The conductivity divided by the width is plotted at the vanishing magnetic field (solid line) and at the magnetic field satisfying $W=0.5R_c$ (dotted line) for the correlation length $\Lambda\ll\lambda_F$. The ratio of the temperature and the averaged level spacing is fixed. The asymptotic formula Eq. (22) (parabolic curve) and Eq. (24) (straight line) are also shown.

Near $y_e/W=0.5$ the amount of positive magnetoresistance is smaller than that at $y_e/W=0$, as has been predicted in the preceding section.

The change in the overall magnetic-field dependence of the resistivity should also be noted. As the confining potential becomes softer, the peak in the positive magnetoresistance becomes sharper and at the same time the resistance starts to have a longer tail at higher magnetic fields. The experimental results by Thornton *et al.*[6] can be best fitted by the result for $y_e\sim 0.3W$. Notice, however, that some caution is necessary to compare the results with experiments due to the presence of localization effects in weak magnetic fields. See the following section for the importance of such localization effects.

Figure 8 shows the energy dependence of the conductivity and contributions from each subband at zero magnetic field. For large y_e/W the amplitude of the quantum oscillation in $\sigma(\varepsilon)$ becomes extremely small. This is a direct consequence of the fact, discussed in the preceding section, that the transition rate from the nth to n'th subband decreases rapidly with increasing $|n-n'|$. At $y_e/W=0.5$ (the parabolic case), the relaxation time or the mean free path is roughly proportional to $(2n-1)^{-1}$, as is given by the approximate result Eq. (26).

IV. NUMERICAL STUDY

A. Model

Effects of boundary-roughness scatterings can be studied numerically within the lattice model used for the

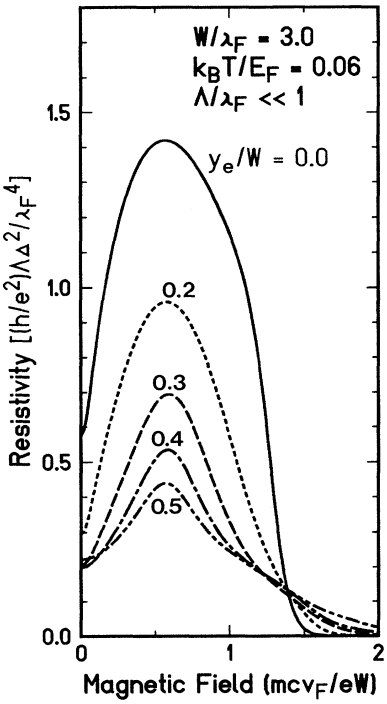

FIG. 7. Calculated magnetoresistance for wires with several confining potentials at $\Lambda\ll\lambda_F$. Wire width is fixed at $W=3\lambda_F$ and an extent of soft walls y_e is varied.

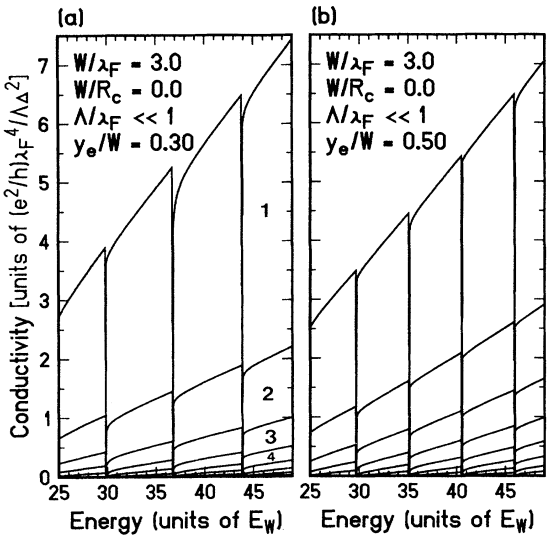

FIG. 8. Calculated conductivity as a function of energy for wires with width $W=3\lambda_F$ for the correlation length $\Lambda \ll \lambda_F$ in the absence of a magnetic field. An extent of soft walls is (a) $y_e/W=0.3$ and (b) $y_e/W=0.5$. The Fermi energy is at $36E_W$ with $E_W=(\hbar^2/2m)(\pi/W)^2$. Contributions from each subband ($n=1,2,\ldots$) are also shown.

study of the localization of edge states.[40] The Hamiltonian is given by

$$\mathcal{H}=\sum_i \varepsilon_i c_i^\dagger c_i - \sum_{i,j} V_{ij} c_i^\dagger c_j \ , \tag{29}$$

where the magnetic field is included in the form of Peierls' phase factor in the nearest-neighbor transfer integral. We have

$$(i_x,i_y|V|i_x+1,i_y)=V\exp[-i(i_y-1)a^2/l^2] \ , \tag{30a}$$

$$(i_x,i_y|V|i_x,i_y+1)=V \quad (i_y=1,2,\ldots,M) \ , \tag{30b}$$

with a the lattice constant and l the magnetic length defined by $(\hbar c/eH)^{1/2}$. For sufficiently large width M, this lattice system corresponds to a continuum system with width W, if we choose the parameters such that

$$\varepsilon_i=-4V, \quad \frac{\hbar^2}{2m}=Va^2, \quad \text{and} \quad W=(M+1)a \ . \tag{31}$$

In order to model effects of boundary roughness we separate the wire into narrow sections. The length of each section takes nd_0 ($n=1,2,\ldots,n_d$) with probability n_d^{-1}. Within each section, the left and right boundaries of the wire are shifted by an amount $\pm n\Delta_0$ ($n=1,2,\ldots,n_\Delta$) with probability q/n_Δ. The probability that each boundary remains unshifted is given by $1-2q$. This gives the correlation function

$$\langle \Delta_+(x)\rangle=\langle \Delta_-(x)\rangle=\langle \Delta_+(x)\Delta_-(x')\rangle=0 \ , \tag{32}$$

$$\langle \Delta_+(x)\Delta_+(x')\rangle=\langle \Delta_-(x)\Delta_-(x')\rangle=\sqrt{\pi}\Delta^2\Lambda g(x-x') \ ,$$

with

$$g(x)=\frac{6}{n_d(n_d+1)(2n_d+1)d_0^2} \times \sum_{n=1}^{n_d}(nd_0-|x|)\Theta(nd_0-|x|) \ ,$$

$$\Lambda=\frac{2}{\sqrt{\pi}n_d(n_d+1)d_0}\sum_{n=1}^{n_d}(nd_0)^2=\frac{2n_d+1}{3\sqrt{\pi}}d_0 \ , \tag{33}$$

$$\Delta^2=\frac{2q}{n_\Delta}\sum_{n=1}^{n_\Delta}(n\Delta_0)^2=\frac{q(n_\Delta+1)(2n_\Delta+1)}{3}\Delta_0^2 \ ,$$

where Θ is a step function defined by $\Theta(t)=1$ for $t>0$ and 0 otherwise. The correlation function satisfies

$$g(0)=\frac{1}{\sqrt{\pi}\Lambda} \quad \text{and} \quad \int_{-\infty}^{+\infty} g(x)dx=1 \ . \tag{34}$$

Because $g(x)$ is different from the Gaussian function, the correlation length Λ can be slightly different from that defined in the preceding section. The present choice guarantees at least that the scattering strength calculated in the Born approximation, determined by the product $\Lambda\Delta^2$, agrees with that given in the preceding section in the limit $\Lambda \ll \lambda_F$.

The transmission coefficients can be calculated using the technique of Green's function (a more detailed description will be given elsewhere)[41] and the conductance is calculated through the multichannel version[42] of Landauer's formula,[32]

$$G=\frac{e^2}{\pi\hbar}\sum_{\mu,\nu}|t_{\mu\nu}|^2 \ , \tag{35}$$

with the transmission coefficient $t_{\mu\nu}$ for outgoing channel μ and incoming channel ν.

B. Results

In numerical calculations we choose the lattice constant a such that $\lambda_F/a \simeq 8.2$. This gives a slight nonparabolicity in the subband dispersion in the absence of a magnetic field but is small enough for the purpose of simulating a continuum system. Further, the magnetic flux passing through the unit cell is at most 2–3 % at the highest magnetic field and therefore the so-called Harper broadening[43,44] is not important. The conductance is obtained by the average over the results for about 10 000 different samples.

Figure 9 gives the results of the numerical calculations for narrow wires with width $W/\lambda_F=2.25$. The correlation length of the roughness is $\Lambda/\lambda_F=0.22$, i.e., still smaller than the Fermi wavelength, and the average height is $\Delta/\lambda_F=0.17$ in (a) and 0.33 in (b). In weak magnetic fields, the conductance always becomes slightly larger than the zero-field value with increasing magnetic field. This increase is due to the reduction of the localization effect in magnetic fields. As a matter of fact, it is more pronounced for stronger boundary roughness [Fig. 9(b)]. With further increase of the field, the conductance starts to decrease, takes a minimum around $W/R_c \sim 1$, and then starts to increase again. This reduction in the conductance around $W/R_c \sim 1$ corresponds to the posi-

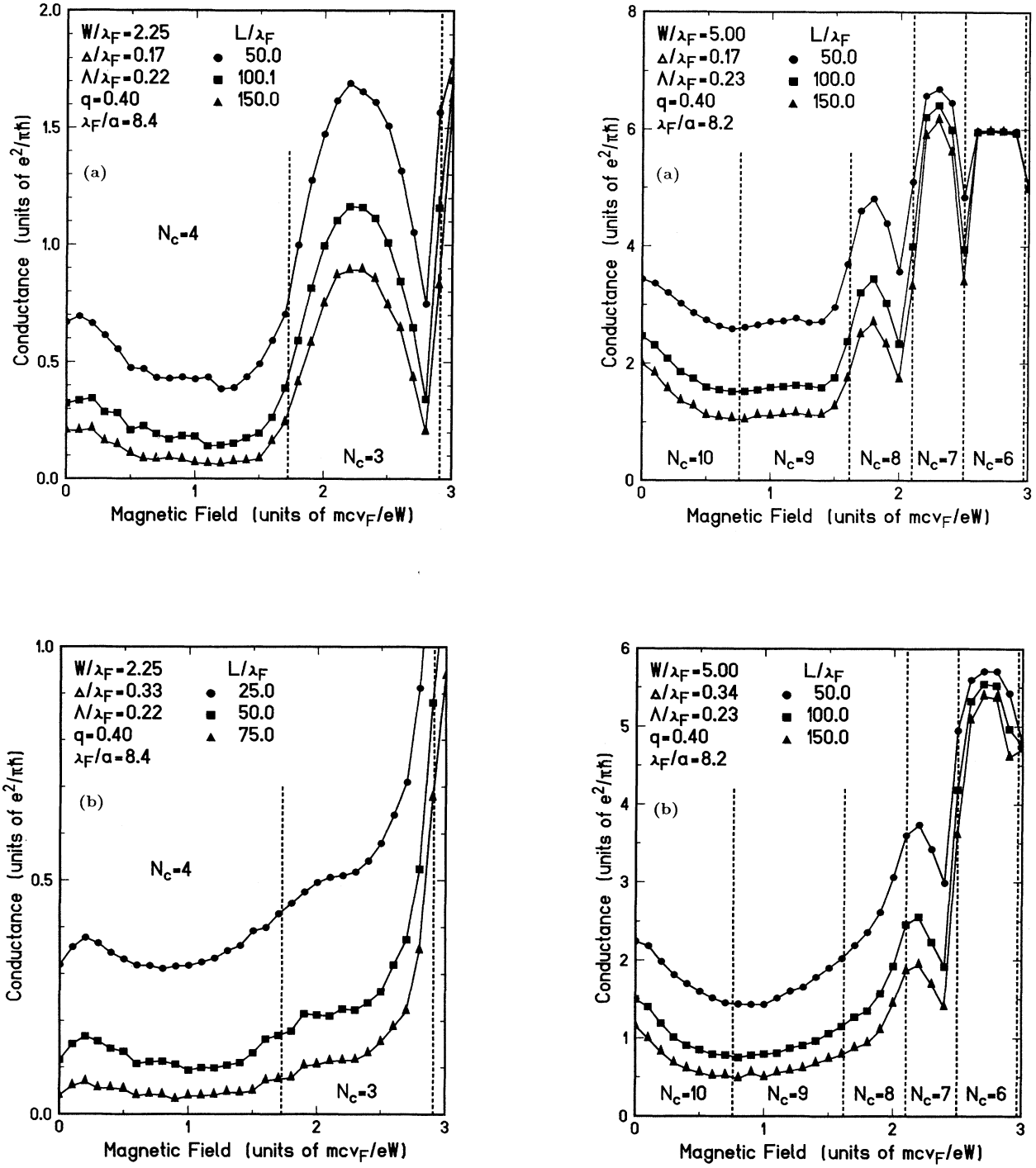

FIG. 9. Calculated conductance as a function of the magnetic field for wires with width $W/\lambda_F=2.25$ and the correlation length of the roughness $\Lambda/\lambda_F=0.22$. (a) $\Delta/\lambda_F=0.17$, $L/\lambda_F=50$, 100, and 150. (b) $\Delta/\lambda_F=0.33$, $L/\lambda_F=25$, 50, and 75. The magnetic depopulation occurs at the fields denoted by the vertical dotted lines and N_c is the number of occupied subbands. The parameters characterizing the lattice are as follows: $M=18$, $q=0.4$, $n_d=n_\Delta=2$, $d_0/a=2$, and $\Delta_0/a=1$ in (a) and $\Delta_0/a=2$ in (b).

FIG. 10. Calculated conductance as a function of the magnetic field for wires with width $W/\lambda_F=5$ and the correlation length of the roughness $\Lambda/\lambda_F=0.23$. (a) $\Delta/\lambda_F=0.17$. (b) $\Delta/\lambda_F=0.34$. The wire length is $L/\lambda_F=50$, 100, and 150. The parameters characterizing the lattice are as follows: $M=40$, $q=0.4$, $n_d=n_\Delta=2$, $d_0/a=2$, and $\Delta_0/a=1$ in (a) and $\Delta_0/a=2$ in (b).

tive magnetoresistance obtained in the preceding section with the use of the Boltzmann transport equation. A quantum oscillation due to the singular one-dimensional density of states appears in strong magnetic fields. Its amplitude decreases for wires with rougher boundaries. In the case of the rough wire, the localization effect is so strong that the conductance around $W/R_c \sim 1$ is still larger than that at the vanishing magnetic field, i.e., the positive magnetoresistance is suppressed.

Figure 10 gives the results for wider wires with $W/\lambda_F = 5$. The correlation length is $\Lambda/\lambda_F = 0.23$ and the average height is $\Delta/\lambda_F = 0.17$ in (a) and 0.34 in (b). For such wide wires, the localization effect is reduced considerably and the conductance always decreases first with the increase of the magnetic field. The maximum length of the wire considered is 150 in units of λ_F, which is about 6 μm for typical $\lambda_F \sim 400$ Å. The conductance takes a minimum around $W/R_c \sim 1$ but its exact position is influenced by the quantum oscillation. For wires with smoother boundary [Fig. 10(a)], the conductance becomes quantized into integer multiples of $e^2/\pi\hbar$ in strong magnetic fields where well-defined edge states are formed and electrons are transmitted through the wire ballistically.

Unfortunately, only a qualitative comparison is possible between these results and those calculated based on the Boltzmann transport equation, partly because of the difference in the correlation function of boundary roughness. The conductance is shown to be modified even in relatively weak fields by the level broadening and to not be proportional to the inverse of $\Lambda\Delta^2$. In the latter calculation, this broadening has not been included and the temperature average has been introduced instead. This leads to a difference in the detailed magnetic-field dependence. Actually the nonzero temperature causes additional effects, such as the contribution of low-energy edge states, leading to the sudden drop of the resistivity in strong magnetic fields and a shift of the resistivity peak to lower fields, as demonstrated in Fig. 4.

The conductance calculated by Landauer's formula is not exactly proportional to the inverse of the length, which is true particularly in strong fields where it is nearly quantized into integer multiples of $e^2/\pi\hbar$ and also in weak fields where the localization effect is important. This is another factor that makes a quantitative comparison difficult but may have partly been overcome if other multichannel versions of Landauer's formula[45–48] are used instead of Eq. (35). Equation (35) has been used for the purpose of seeing whether characteristic features of the positive magnetoresistance are reproduced within the framework of the transmission approach. It has been demonstrated above that qualitatively a similar positive magnetoresistance is predicted for wide wires by both Boltzmann and transmission approaches, showing that the Boltzmann transport equation can be safely used for the study of the magnetoresistance in the present system.

V. SUMMARY AND CONCLUSION

In conclusion, we have studied the effects of boundary-roughness scatterings on the magnetoresistance of quantum wires, using the Boltzmann transport equation. Roughness gives rise to a strong positive magnetoresistance, on which quantum oscillations are superposed at low temperatures. This positive magnetoresistance is explained by the disappearance of the singularly long mean free paths of electrons in the lowest few subbands present at zero magnetic field. The effect is less prominent for narrower wires and vanishes when the width is less than the Fermi wavelength. The correlation length of the roughness, which does not appear in the classical theory, is also an important parameter. Roughness with a large correlation length gives no positive magnetoresistance because of dominant forward scattering. The magnetoresistance is affected also by the shape of the confining potential and tends to be more sharply peaked at its maximum value when the confinement becomes softer.

The magnetoresistance has also been studied numerically with the use of Landauer's conductance formula. In narrow wires, the localization effect is important and leads to the negative magnetoresistance in weak magnetic fields ($W/R_c \lesssim 0.1$). For very rough wires, the positive magnetoresistance can be suppressed by the localization effect. With the increase of the wire width, however, the localization effect becomes less and less important and a clear positive magnetoresistance is obtained. The position of the resistance peak depends on whether or not the quantum oscillation due to the singular one-dimensional density of states is smeared out.

ACKNOWLEDGMENTS

This work is supported in part by the Industry-University Joint Research Program "Mesoscopic Electronics" and by a Grant-in-Aid for Scientific Research on Priority Area "Electron Wave Interference Effects in Mesoscopic Structures" from the Ministry of Education, Science and Culture.

APPENDIX: PROOF OF EQ. (16)

By making integration by parts, we have

$$Y^{\pm}_{\beta\alpha} = \pm\frac{2m}{\hbar^2}\int_{\pm W_0/2}^{\pm\infty} dy \left[\frac{\partial\eta_\beta}{\partial y}\eta_\alpha + \eta_\beta\frac{\partial\eta_\alpha}{\partial y}\right] V(y) \ . \qquad \text{(A1)}$$

Using the Schrödinger equation with Hamiltonian Eq. (1), we obtain

$$Y^{\pm}_{\beta\alpha} = \pm\int_{\pm W_0/2}^{\pm\infty} dy \frac{\partial}{\partial y}\left[\frac{\partial\eta_\beta}{\partial y}\frac{\partial\eta_\alpha}{\partial y}\right] \pm\int_{\pm W_0/2}^{\pm\infty} dy \left[\frac{\partial\eta_\beta}{\partial y}\eta_\alpha g_\alpha + g_\beta\eta_\beta\frac{\partial\eta_\alpha}{\partial y}\right] , \qquad \text{(A2)}$$

with

$$g_\alpha = \frac{2m}{\hbar^2}\left[\varepsilon_\alpha - \frac{\hbar^2 k_\alpha^2}{2m} - \tfrac{1}{2}m\omega_c^2 y^2 + \hbar\omega_c k_\alpha y\right], \quad \text{(A3)}$$

where $\omega_c = eH/mc$. The first term of Eq. (A2) gives the formula Eq. (16). When the confining potential approaches the hard wall, $\eta(y)$ and $\partial\eta/\partial y$ in the integrand of the second term are negligible except in the vicinity of $y = \pm W_0/2$ and the slowly varying function $g(y)$ can be replaced by $g(\pm W_0/2)$. Therefore we have

$$\left|\int_{\pm W_0/2}^{\pm\infty} dy \frac{\partial\eta_\beta}{\partial y}\eta_\alpha\right| < \left|\int_{\pm W_0/2}^{\pm\infty} dy \frac{\partial\eta_\beta}{\partial y}\right| |\eta_\alpha(\pm W_0/2)| = |\eta_\beta(\pm W_0/2)||\eta_\alpha(\pm W_0/2)|, \quad \text{(A4)}$$

which vanishes in the limit of the hard-wall confining potential.

[1] G. Timp, A. M. Chang, P. M. Mankiewich, R. E. Behringer, J. E. Cunningham, T. Y. Chang, and R. E. Howard, Phys. Rev. Lett. **59**, 732 (1987).

[2] M. L. Roukes, A. Scherer, S. J. Allen, Jr., H. G. Craighead, R. M. Ruthen, E. D. Beebe, and J. P. Harbison, Phys. Rev. Lett. **59**, 3011 (1987).

[3] C. J. B. Ford, S. Washburn, M. Büttiker, C. M. Knoedler, and J. M. Hong, Phys. Rev. Lett. **62**, 2724 (1989).

[4] G. Timp, H. U. Baranger, P. de Vegvar, J. E. Cunningham, R. E. Howard, R. E. Behringer, and P. M. Mankiewich, Phys. Rev. Lett. **60**, 2081 (1988).

[5] Y. Takagaki, K. Gamo, S. Namba, S. Takaoka, K. Murase, S. Ishida, K. Ishibashi, and Y. Aoyagi, Solid State Commun. **68**, 1051 (1988); **69**, 811 (1989).

[6] T. J. Thornton, M. L. Roukes, A. Scherer, and B. P. Van de Gaag, Phys. Rev. Lett. **63**, 2128 (1989).

[7] K. Forsvoll and I. Holwech, Philos. Mag. **9**, 435 (1964).

[8] J. M. Ziman, *Electrons and Phonons* (Oxford University Press, London, 1960), pp. 451–482.

[9] R. G. Chambers, in *The Physics of Metals 1. Electrons*, edited by J. M. Ziman (Cambridge University Press, Cambridge, 1969), pp. 175–249.

[10] T. J. Coutts, *Electrical Conduction in Thin Metal Films* (Elsevier, Amsterdam, 1974), pp. 149–204.

[11] A. B. Pippard, *Magnetoresistance in Metals* (Cambridge University Press, Cambridge, 1989), pp. 196–236.

[12] K. Fuchs, Proc. Cambridge Philos. Soc. **34**, 100 (1938).

[13] D. K. C. MacDonald and K. Sarginson, Proc. R. Soc. (London) Ser. A **203**, 223 (1950).

[14] M. Ya. Azbel, Zh. Eksp. Teor. Fiz. **44**, 1262 (1963) [Sov. Phys.—JETP **17**, 851 (1963)].

[15] E. Ditlefsen and J. Lothe, Philos. Mag. **14**, 759 (1966).

[16] A. V. Chaplik and M. V. Éntin, Zh. Eksp. Teor. Fiz. **55**, 990 (1968) [Sov. Phys.—JETP **28**, 514 (1969)].

[17] Z. Tešanović, M. V. Jarić, and S. Maekawa, Phys. Rev. Lett. **57**, 2760 (1986).

[18] N. Trivedi and N. W. Ashcroft, Phys. Rev. B **38**, 12 298 (1988).

[19] D. Calecki, Phys. Rev. B **42**, 6906 (1990).

[20] R. E. Prange and Tsu-Wei Nee, Phys. Rev. **168**, 779 (1968).

[21] For effects of boundary roughness on the electron transport and their theoretical treatment, see, for example, T. Ando, A. B. Fowler, and F. Stern, Rev. Mod. Phys. **54**, 437 (1982).

[22] M. V. Éntin, Fiz. Tverd. Tela **11**, 958 (1969) [Sov. Phys.—Solid State **11**, 781 (1969)].

[23] Y. C. Cheng, Surf. Sci. **27**, 663 (1971); J. Jpn. Soc. Appl. Phys. Suppl. **41**, 173 (1972); Surf. Sci. **40**, 433 (1973); Jpn. J. Appl. Phys. Suppl. **2**, Pt. 2, 363 (1974).

[24] Y. C. Cheng and E. A. Sullivan, J. Appl. Phys. **44**, 923 (1973); **44**, 3619 (1973); Surf. Sci. **34**, 717 (1973).

[25] Y. Matsumoto and Y. Uemura, Jpn. J. Appl. Phys. Suppl. **2**, Pt. 2, 367 (1974).

[26] T. Ando, J. Phys. Soc. Jpn. **43**, 1616 (1977).

[27] S. Mori and T. Ando, Phys. Rev. B **19**, 6433 (1979).

[28] S. Mori and T. Ando, J. Phys. Soc. Jpn. **48**, 865 (1980).

[29] A. Gold, Phys. Rev. B **35**, 723 (1987).

[30] H. Sakaki, T. Noda, K. Hirakawa, M. Tanaka, and T. Matsusue, Appl. Phys. Lett. **51**, 1934 (1987).

[31] H. Akera and T. Ando, Phys. Rev. B **41**, 11 967 (1990).

[32] R. Landauer, IBM J. Res. Dev. **1**, 223 (1957); Philos. Mag. **21**, 863 (1970).

[33] S. E. Laux, D. J. Frank, and F. Stern, Surf. Sci. **196**, 101 (1988).

[34] D. A. Wharam, U. Ekenberg, M. Pepper, D. G. Hasko, H. Ahmed, J. E. F. Frost, D. A. Ritchie, D. C. Peacock, and G. A. C. Jones, Phys. Rev. B **39**, 6283 (1989).

[35] K.-F. Berggren, G. Roos, and H. van Houten, Phys. Rev. B **37**, 10 118 (1988).

[36] See, for example, E. D. Siggia and P. C. Kwok, Phys. Rev. B **2**, 1024 (1970).

[37] H. Mori, Progr. Theor. Phys. **33**, 423 (1965); **34**, 399 (1965).

[38] W. Götze and P. Wölfle, Phys. Rev. B **6**, 1226 (1972).

[39] J. A. Nixon and J. H. Davies, Phys. Rev. B **41**, 7929 (1990).

[40] T. Ando, Phys. Rev. B **42**, 5626 (1990).

[41] T. Ando (unpublished).

[42] D. S. Fisher and P. A. Lee, Phys. Rev. B **23**, 6851 (1981).

[43] P. G. Harper, Proc. Phys. Soc. London Sec. A **68**, 874 (1955).

[44] D. R. Hofstadter, Phys. Rev. B **14**, 2239 (1976).

[45] P. W. Anderson, D. J. Thouless, E. Abrahams, and D. S. Fisher, Phys. Rev. B **22**, 3519 (1980).

[46] P. W. Anderson, Phys. Rev. B **23**, 4828 (1981).

[47] M. Ya. Azbel, J. Phys. C **14**, L225 (1981).

[48] M. Büttiker, Y. Imry, R. Landauer, and S. Pinhas, Phys. Rev. B **31**, 6207 (1985).